Finite-temperature study of Bose-Fermi superfluid mixtures

B. Ramachandhran, S. G. Bhongale, and H. Pu

Phys. Rev. A **83**, 033607 — Published 10 March 2011

DOI: 10.1103/PhysRevA.83.033607

Finite-Temperature Study of Bose-Fermi Superfluid Mixtures

B. Ramachandhran,[1] S. G. Bhongale,[1,2] and H. Pu[1]

[1]*Department of Physics & Astronomy, and Rice Quantum Institute, Rice University, Houston, TX 77005, USA*
[2]*Department of Physics & Astronomy, George Mason University, MS 3F3, Fairfax, VA 22030*

Ultra-cold atom experiments offer the unique opportunity to study mixing of different types of superfluid states. Our interest is in superfluid mixtures comprising particles with different statistics– Bose and Fermi. Such scenarios occur naturally, for example, in dense QCD matter. Interestingly, cold atomic experiments are performed in traps with finite spatial extent, thus critically destabilizing the occurrence of various homogeneous phases. Critical to this analysis is the understanding that the trapped system can undergo phase separation, resulting in a unique situation where phase transition in either species (bosons or fermions) can overlap with the phase separation between possible phases. In the present work, we illustrate how this intriguing interplay manifests in an interacting 2-species atomic mixture – one bosonic and another fermionic with two spin components – within a realistic trap configuration. We further show that such interplay of transitions can render the nature of the ground state to be highly sensitive to the experimental parameters and the dimensionality of the system.

PACS numbers: 67.85.Pq, 67.85.-d, 67.85.Lm

I. INTRODUCTION

Ultra-cold trapped-atom experiments offer the unique possibility to understand many-body physics beyond what can be explored in typical condensed matter settings [1]. Essentially, they provide clean many-body systems in which attributes like density, dimensionality and interactions, may be controlled with commendable precision [2–5]. As a result, from a theoretical perspective, there are broadly two kinds of challenges: (1) investigate configurations appropriate for emulating many-body theory models, thereby allowing for a systematic verification of claims made in the condensed matter context, and (2) investigate new configurations extremely difficult to realize in material settings. While the former program has proved quite successful with demonstrations of, for example, Mott insulator to superfluid transition with ultra-cold ^{87}Rb atoms in an optical lattice [6], the latter is just beginning to attract attention with several new experiments comprising degenerate mixtures of bosons and fermions, of same or different species being set up [7, 8]. A potentially rich scenario in this context is provided by an atomic mixture comprising superfluids of two kinds- bosonic and fermionic. Studying this system may also have strong implications for, say nuclear physics, as a recent proposal investigates the intriguing possibility of simulating dense QCD matter with superfluid atomic mixtures [9]. Further, considering that in condensed matter setting, the analogous ^{3}He-^{4}He superfluid mixture is difficult to realize [10], achieving Bose-Fermi superfluid mixtures with ultra-cold atoms maybe an important step towards understanding corresponding occurrences in a broader context.

In analyzing experiments with ultra-cold Bose-Fermi mixtures, it is important to understand the effects of inhomogeneity due to traps. These effects are at the heart of determining the stability of possible thermodynamic phases in a given experiment. To this end, we construct the finite-temperature phase diagram of an interacting 3-dimensional (3-d) mixture comprising of two fermions (spin $\uparrow$ & $\downarrow$) of one species and a bosons of another. To draw such a phase diagram, it is important to understand the interplay between the following two phenomena: (1) phase transition that occurs near a critical temperature where suddenly an order parameter corresponding to one of the species nucleates. In fact, the critical temperature of such a transition may itself depend intricately on the state of the second species. Moreover, the already nucleated phase may subsequently be drastically affected in a certain region of trap due to the nucleation of a new phase, corresponding to the second species, as the system is further cooled and crosses below a lower critical temperature. (2) phase separation between possible phases, a phenomenon unique to trapped configurations. It also implies that the trap potential can simultaneously accommodate one or more of the phases as determined by the experimental parameters. Thus, remarkably what phase/phases will be observed will critically depend on the trap geometry. This, in fact is a very important observation implying the possibility of tuning the trap parameters such that a desired density profile is observed only if a certain phase has nucleated. On top of all this, the dimensionality of the trapped system, whether we consider a 3-d or a 1-d trap, will also largely determine what phase is energetically favorable for phase separation.

While various possibilities discussed above exist and some insight may be borrowed from previous studies on pure Bose and Fermi superfluids, the intrinsically new nature of Bose-Fermi superfluid mixtures strongly motivates us to derive a framework within which an elaborate finite temperature phase diagram can be generated. Also, such finite temperature studies comprising interacting fermions have never been performed in the past. The paper is organized as follows. In Sec. II, we first review the theory for analyzing the thermodynamic instabilities

of the Bose-Fermi mixture. While the technique is quite standard and maybe found elsewhere, to our knowledge this is the first instance where it has been applied for deriving the finite temperature phase diagram of the inhomogeneous mixture comprising of bosons and fermions, both in the superfluid phase. As discussed in the previous paragraphs, the trap introduces multiple scenarios that are new to these systems making the analysis complicated. Therefore as a warmup, in Sec. III A we illustrate our method by first considering the simplest case of the $T = 0$ superfluid mixture in 3-d. The finite temperature phase diagram for the 3-d Bose Fermi mixture will be derived in Sec. III B. Finally, in Sec. IV, we will discuss the implication of the phase diagram for a *trapped* Bose-Fermi mixture by introducing a spatially varying chemical potential in the spirit of a Local Density Approximation (LDA), followed by brief discussion of the dependance on dimensionality in Sec. V.

II. THEORY

We begin by writing the Hamiltonian for the interacting Bose-Fermi mixture in the form

$$\hat{H} = \underbrace{\hat{H}_b - \mu_b \hat{N}_b}_{\hat{\mathcal{H}}_b} + \underbrace{\hat{H}_f - \mu_f \hat{N}_f + U_{bf} \hat{N}_b \hat{N}_f}_{\hat{\mathcal{H}}_{bf}}, \quad (1)$$

where the subscript b (f) stands for bosons (fermions), μ's represent corresponding chemical potentials, $\hat{N}$'s the corresponding number operators and U_{bf} denotes the interaction energy between bosons and fermions. Our interest is in studying this interacting Bose-Fermi mixture in the vicinity of the superfluid critical temperature T_c of the fermions. Of course, it is true that the T_c itself will be modified due to the presence of Bose component. Further, the phase of fermions may modify the critical temperature for the condensation of the Bose component, T_{BEC}. Thus, while the general problem is indeed complicated, we focus our attention on the situation when T_{BEC} is much greater than T_c, typically the case in most trapped experiments [11]. This allows us to work in the Thomas-Fermi limit of the Bose component by neglecting its kinetic energy. We represent the contact interaction strength between a pair of bosons as $\lambda_b = U_b\, V = 4\pi\hbar^2 a_b/m$, where U_b is the interaction energy of bosons, V is the volume, a_b is the s-wave boson-boson scattering length, assumed to be positive implying repulsive interactions, and m is the mass of bosonic atom. For large boson number N_b, total pairs of bosons is approximately $N_b^2/2$ and hence, $\hat{H}_b$ is simply a constant given by $U_b N_b^2/2$. Thus, the contribution to the free energy density arising from just the bosonic component is

$$f_b = \langle \hat{\mathcal{H}}_b \rangle = \lambda_b \frac{n_b^2}{2} - \mu_b\, n_b, \quad (2)$$

where $n_b = N_b/V$ is the boson density.

Now, we focus on the $\hat{\mathcal{H}}_{bf}$ part of the Hamiltonian and write it explicitly in second quantized form as

$$\hat{\mathcal{H}}_{bf} = \sum_{k,\sigma} (\varepsilon_k - \mu_f)\, c^\dagger_{k,\sigma} c_{k,\sigma} + \lambda_f \sum_{k,k',q} c^\dagger_{k+q,\uparrow}\, c^\dagger_{-k,\downarrow} c_{-k'+q,\downarrow}\, c_{k',\uparrow} + \lambda_{bf}\, n_b \sum_{k,\sigma} c^\dagger_{k,\sigma} c_{k,\sigma}. \quad (3)$$

Here $\varepsilon_k = \hbar^2 k^2/2m$ and $c^\dagger_{k,\sigma}(c_{k,\sigma})$ is the creation (annihilation) operator for a fermion with momentum k and spin σ. Further, the boson-fermion interaction, which is typically short range, is described by a δ-potential contact interaction with strength given by $\lambda_{bf} = 2\pi\hbar^2 a_{bf}/\mu_m$, where a_{bf} is the corresponding s-wave scattering length and μ_m is the reduced mass of the boson-fermion system. Here we will confine our analysis to the repulsive regime with $a_{bf} > 0$. Similarly, we describe the fermion-fermion interaction by the contact interaction strength $\lambda_f = 4\pi\hbar^2 a_f/m$, where a_f is the corresponding s-wave scattering length. Here, since the interaction is s-wave, only unequal-spin fermions interact. Also, we are interested in the superfluid regime, which occurs for attractive interactions, thus we assume $a_f < 0$. Now, in the superfluid state with BCS-type pairing [12, 13], the center-of-mass momentum, q, of the Cooper pair is set to zero allowing $\hat{\mathcal{H}}_{bf}$ to be simply

$$\hat{\mathcal{H}}_{bf} = \sum_{k,\sigma} \xi_k\, c^\dagger_{k,\sigma} c_{k,\sigma} - |\lambda_f| \sum_{k,k'} c^\dagger_{k,\uparrow}\, c^\dagger_{-k,\downarrow} c_{-k',\downarrow}\, c_{k',\uparrow}, \quad (4)$$

with $\xi_k = \varepsilon_k - \mu_f + \lambda_{bf} n_b$. One can immediately notice that this is just the usual BCS Hamiltonian with a modified chemical potential, hence can be diagonalized with the usual Bogoliubov transformation [14]. Firstly, defining the mean-field order parameter $\Delta = |\lambda_f| \sum_{k'} \langle c_{-k',\downarrow}\, c_{k',\uparrow} \rangle$ and its complex conjugate Δ^*, we write $\hat{\mathcal{H}}_{bf}$ as

$$\hat{\mathcal{H}}_{bf} \stackrel{M.F}{=} \sum_k \xi_k \big(c^\dagger_{k,\uparrow} c_{k,\uparrow} + c^\dagger_{k,\downarrow} c_{k,\downarrow} \big) + \frac{|\Delta|^2}{|\lambda_f|} - \big(\Delta^* \sum_{k'} c_{-k',\downarrow}\, c_{k',\uparrow} + \Delta \sum_k c^\dagger_{k,\uparrow}\, c^\dagger_{-k,\downarrow} \big). \tag{5}$$

Re-writing the above in terms of the *Nambu spinor* $\Psi^\dagger_k = (c^\dagger_{k,\uparrow}, c_{-k,\downarrow})$ and its hermitian conjugate Ψ_k, we have

$$\hat{\mathcal{H}}_{bf} = \sum_k \Psi^\dagger_k \begin{pmatrix} \xi_k & -\Delta \\ -\Delta^* & -\xi_k \end{pmatrix} \Psi_k + \sum_k \xi_k + \frac{|\Delta|^2}{|\lambda_f|}. \tag{6}$$

Now the Bogoliubov transformation immediately gives

$$\begin{aligned} \hat{\mathcal{H}}_{bf} &= \sum_k \left(\alpha^\dagger_{k,\uparrow}, \alpha_{-k,\downarrow} \right) \begin{pmatrix} E^+_k & 0 \\ 0 & E^-_k \end{pmatrix} \begin{pmatrix} \alpha_{k,\uparrow} \\ \alpha^\dagger_{-k,\downarrow} \end{pmatrix} \\ &+ \sum_k \xi_k + \frac{\Delta^2}{|\lambda_f|}, \end{aligned} \tag{7}$$

where the eigenenergies are $E^\pm_k = \pm\sqrt{\xi^2_k + \Delta^2}$ and Δ is assumed real [15]. The operator $\alpha^\dagger_{k,\uparrow}$ ($\alpha_{k,\uparrow}$) creates (annihilates) Bogoliubov quasiparticles that are distributed according to the Fermi-Dirac distribution $f_k = 1/(1+e^{\beta E_k})$ with $\beta = 1/k_B T$. Thus the relevant thermodynamic potential is given by

$$\langle \hat{\mathcal{H}}_{bf} \rangle - TS = \sum_k (\xi_k - E_k) + \frac{\Delta^2}{|\lambda_f|} - \frac{2}{\beta} \sum_k \ln\left(1 + e^{-\beta E_k}\right) \tag{8}$$

where S is the entropy. The derivations and mean-field analysis presented henceforth is quantitatively exact only when the interactions are weak. Our analysis is only qualitatively correct in the strong interaction limit, where a strong-coupling theory presented along the lines of Ref. [16] would be quantitatively more accurate.

A. Free energy, Equilibrium and dynamical stability conditions

Free energy density of the interacting mixture comprising of bosons and fermions, both in the superfluid state, can now be written from Eqs. (2) and (8):

$$f = \frac{\lambda_b n_b^2}{2} - \mu_b\, n_b + \sum_k (\xi_k - E_k) + \frac{\Delta^2}{|\lambda_f|} - \frac{2}{\beta} \sum_k \ln\left(1 + e^{-\beta E_k}\right).$$

As one can immediately notice, f depends on numerous parameters: interaction strengths $\lambda_{\{b,f,bf\}}$ (in-turn, the scattering lengths $a_{\{b,f,bf\}}$), particle densities $n_{\{b,f\}}$, chemical potentials $\mu_{\{b,f\}}$, BCS superfluid order parameter Δ and temperature T. It is quite evident that the phase space of this interacting mixture is huge and thus an exhaustive study is impossible. However, noticing the fact that not all of these parameters are independent, we adopt the following scheme that was first introduced in Ref. [17], allowing us to investigate the experimentally relevant region of the phase space: (1) fix parameters λ_b, λ_{bf} and μ_f and perform our analysis at fixed values of T [18]; (2) we project the multi-dimensional phase diagram in the $\{n_b, \Delta\}$ phase space; (3) the remaining dependent parameters μ_b, n_f and λ_f are determined by the equilibrium stability conditions to be derived below.

(1) First derivative conditions: First of these is the Gap equation obtained as the extremum of f with respect to Δ and provides the self-consistent value of the interaction strength parameter λ_f:

$$\frac{\partial f}{\partial \Delta} = 0 \implies \frac{1}{|\lambda_f|} = \sum_k \frac{1}{2\, E_k} \tanh\left(\frac{\beta E_k}{2}\right).$$

However, in three dimensions, the momentum sum in the above expression diverges, an artifact of the contact interaction approximation. This unphysical effect is easily eliminated by an appropriate regularizing prescription. One of the easiest and convenient methods is to subtract the diverging piece:

$$\frac{1}{|\lambda_f|} = \frac{m}{4\pi\hbar^2 |a_f|} = \sum_k \frac{1}{2\, E_k} \tanh\left(\frac{\beta E_k}{2}\right) - \frac{1}{2\, \varepsilon_k}. \tag{9}$$

Correspondingly, we upgrade the free energy f to the regularized $f_{\rm reg}$ such that the extremum condition automatically reproduces the regularized version of the Gap equation [19]

$$\begin{aligned} f_{\rm reg}(n_b, \Delta) &= \lambda_b \frac{n_b^2}{2} - \mu_b\, n_b + \sum_k (\xi_k - E_k + \frac{\Delta^2}{2\, \varepsilon_k}) \\ &+ \frac{\Delta^2}{|\lambda_f|} - \frac{2}{\beta} \sum_k \ln\left(1 + e^{-\beta E_k}\right). \end{aligned} \tag{10}$$

The above step is essential for our case since we will be eventually interested not only in the stability of the Fermi system but that of the combined Bose-Fermi system. The presence of bosons affects the self-consistent value of λ_f, through the combination $\lambda_{bf}\, n_b$. Next we consider the variation with respect to the fermion chemical potential μ_f. This produces the familiar equation determining the fermion number density n_f:

$$\frac{\partial (f_{\rm reg} + \mu_f\, n_f)}{\partial \mu_f} = 0 \implies n_f = \sum_k 1 - \frac{\xi_k}{E_k} \tanh\left(\frac{\beta E_k}{2}\right). \tag{11}$$

Finally, the last of dependent parameters, the boson chemical potential μ_b is determined by minimizing $f_{\rm reg}$ with respect to the boson density. This leads to the modified Thomas-Fermi equation given by

$$\partial f_{\rm reg}/\partial n_b = 0 \implies \mu_b = \lambda_b n_b + \lambda_{bf} n_f. \qquad (12)$$

(2) Second derivative conditions: The second derivatives at the extremum points derived above provide the dynamical stability criterion for the mixture via positive definiteness of the Hessian matrix $\mathcal{M}$. The relevant Hessian matrix elements are:

$$\mathcal{M}_{11} = \frac{\partial^2 f_{\rm reg}}{\partial n_b^2} = \lambda_b - \lambda_{bf}^2 \sum_k \frac{\Delta^2}{E_k^3} \tanh(\frac{\beta E_k}{2}) - \frac{\beta}{2}\frac{\xi_k^2}{E_k^2} \mathrm{sech}(\frac{\beta E_k}{2})^2; \qquad (13)$$

$$\mathcal{M}_{22} = \frac{\partial^2 f_{\rm reg}}{\partial \Delta^2} = \sum_k \frac{\Delta^2}{E_k^3} \tanh(\frac{\beta E_k}{2}) - \frac{\beta}{2}\frac{\Delta^2}{E_k^2} \mathrm{sech}(\frac{\beta E_k}{2})^2; \qquad (14)$$

$$\mathcal{M}_{12} = \mathcal{M}_{21} = \frac{\partial^2 f_{\rm reg}}{\partial \Delta\, \partial n_b} = \lambda_{bf} \sum_k \frac{\Delta\, \xi_k}{E_k^3} \tanh(\frac{\beta E_k}{2}) - \frac{\beta}{2}\frac{\Delta\, \xi_k}{E_k^2} \mathrm{sech}(\frac{\beta E_k}{2})^2. \qquad (15)$$

III. FINITE TEMPERATURE PHASE DIAGRAM

For illustrative purposes, we start with a brief discussion of the zero-temperature phase diagram. Throughout, we follow the scheme outlined in Sec. II A to construct all the phase diagrams.

A. Zero-Temperature limit

This is simply derived by taking the $T = 0$ limit of Eqs. (9)-(15). In the phase diagram shown in Fig. 1(a), the solid (green) curve represents the boundary of the dynamically stable region above it, separating the unstable region below. However, it is important to note that, in the phase diagram the interaction parameter λ_f is determined self-consistently from the Gap equation. Thus in any single experimental realization, only a small portion, corresponding to a fixed λ_f, of the above phase space is accessible. In our analysis, we choose a value of λ_f (corresponding to $1/k_f\, a_f = -1.10$) such that pure fermions are in the BCS superfluid regime. This corresponds to a BCS superfluid critical temperature of $T_c = 0.11\, T_f$, with T_f being the Fermi temperature [20]. It is however important to note that $T_{c,\rm mix}$, the BCS transition temperature of fermions in the presence of bosons, is modified by the presence of the factor $\lambda_{bf}\, n_b$ in the effective fermion chemical potential. Further, the dependence is such that $T_{c,\rm mix} \leq T_c$ and the equality is satisfied when $\lambda_{bf} n_b \to 0$.

Points in the phase space that correspond to this fixed value of λ_f is shown by the dashed (blue) contour C in Fig. 1(a). The crossing of this contour with the dynamical stability contour indicates the phase space point at which the homogeneous mixture enters the dynamically stable region. However, for the homogeneous mixture to be the stable ground state, mechanical stability condition should also be satisfied on top of the dynamical stability condition. This additional criterion is exclusively present due to the spatial inhomogeneity intrinsic in trapped-atom setups. By mechanical stability, we mean that the free energy of the homogeneous mixture should be less than the free energy of the pure bosonic phase or the pure fermionic phase along the contour C. The value of the latter is a constant, since λ_f is fixed along C. Free energy of pure bosons along C is given by

$$f_b[C] = -\frac{\mu_b^2[C]}{2\,\lambda_b} \qquad (16)$$

where, $\mu_b[C]$ is the boson chemical potential along C.

The plot of Fig. 1(b) shows the comparison of free energies mentioned above. The free energy of the pure fermionic phase and that of the homogeneous Bose-Fermi mixture along C are represented by the solid and the dashed lines respectively. The free energy of pure bosons is much higher than the others and hence bosons do not phase separate out of the mixture. Actually this observation is a general property of the phase space of a 3-dimensional Bose-Fermi mixture. The filled circle (red) represents the critical point along contour C, at which the free energy of the homogeneous mixture is lower than that of pure fermions, i.e., the critical point at which the homogeneous mixture enters a region of both dynamical and mechanical stability. This implies that, for the specific experimental realization considered here, up until this critical point pure fermions phase separate out of the mixture, while above the critical point the Bose-

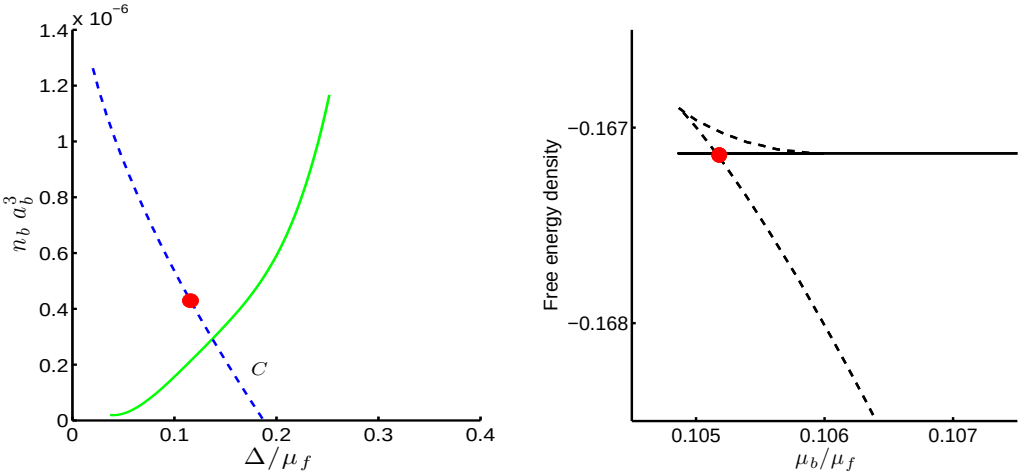

FIG. 1: (Color online) (a) Phase diagram of the Bose-Fermi superfluid mixture at $T = 0$ [21]. Solid (green) curve is the dynamical stability contour while the dashed (blue) contour C denotes points in phase space with a fixed value of λ_f such that $T_c = 0.11\, T_f$. The filled (red) circle represents the critical point, for this specific experimental realization, at which the homogeneous mixture enters the dynamically and mechanically stable region. (b) Plot of the free energy densities of pure fermions (solid) and the homogeneous mixture (dashed) against $\mu_b[C]$. Free energy of homogeneous mixture is lower than that of pure fermions only beyond the critical point represented by the filled (red) circle. Here, free energy density is a dimensionless quantity [22].

Fermi superfluid exists as a stable mixed phase.

B. Finite-Temperature scenario

We begin the discussion of the finite temperature case by first emphasizing some of the generic aspects of such a phase diagram as depicted in the schematic of Fig. 2.

1. *Generic features*

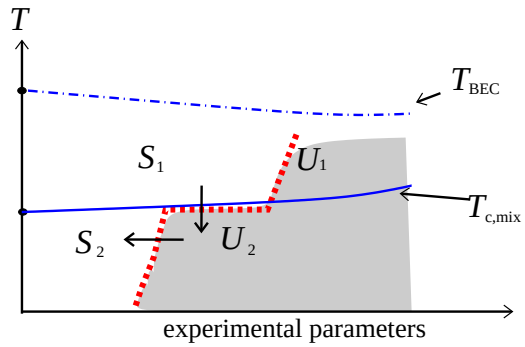

FIG. 2: (Color online) Schematic depicting possible first-order transitions occurring in Bose-Fermi mixtures across $T_{c,\mathrm{mix}}$. Horizontal axis denotes the $\mathbb{R}^5$ phase space of experimental parameters defined by $\{\lambda_b, \lambda_{bf}, \mu_f, n_b, \Delta\}$.

Similar to the above illustration of the zero-temperature limit, we analyze the stability of the superfluid Bose-Fermi mixture in the vicinity of BCS critical temperature for a wide range of temperature and other parameter values. As mentioned earlier in Sec. II A, the phase space is huge (5-dimensional) allowing for complicated boundaries between stable (S_i) and unstable (U_i) regions of the homogeneous mixture. Before proceeding to the detailed quantitative finite temperature phase diagram in Fig. 3, we therefore summarize our findings by pointing out the broad features, as depicted in Fig. 2. In a certain projected subspace, the homogeneous Bose-Fermi mixture becomes dynamically and/or mechanically unstable towards phase separation through a first-order transition $S_1 \to U_2$, when cooled across $T_{c,\mathrm{mix}}$. The tunability of experimental parameters further allows us to access the $U_2 \to S_2$ transition at some fixed temperature below $T_{c,\mathrm{mix}}$. We also observe the existence of a parameter regime where the homogeneous mixture remains unstable across $T_{c,\mathrm{mix}}$ going from $U_1 \to U_2$. If fermions phase separate out of the unstable regions, then along the phase space boundary between U_1 and U_2, and that between U_2 and S_1, $T_{c,\mathrm{mix}}$ is essentially T_c. Thus, in short, the Bose-Fermi mixture exhibits rich mixing-demixing physics in the vicinity of the BCS critical temperature. Particularly interesting is the parameter regime exhibiting the first-order transitions $S_1 \to U_2 \to S_2$, which shows how the already condensed bosons affect the nucleation of fermions when cooled across the critical temperature, thereby clearly indicating direct implication for the observation of Fermi superfluidity in trapped mixtures. We therefore address this part of the phase space in more detail.

2. Quantitative features

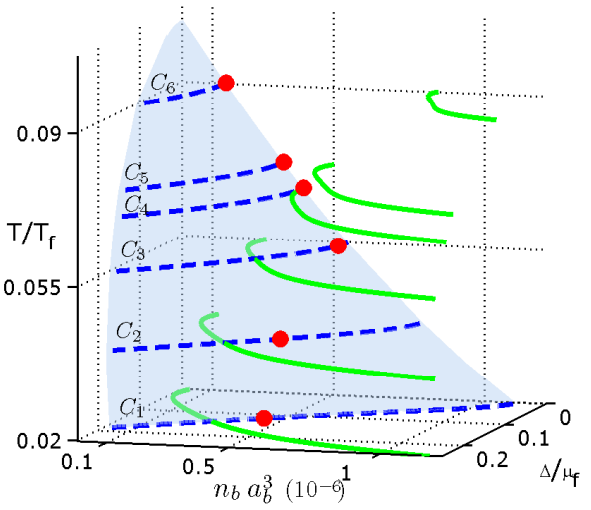

FIG. 3: (Color online) Phase diagram of the Bose-Fermi superfluid mixture at temperatures $T_c > T$. Solid (green) curves show dynamical stability criteria and the (blue) surface represents points of fixed λ_f, such that $T_c = 0.11\ T_f$ [20, 21]. Dashed (blue) curves C_i are contours of fixed temperature T_i along this surface and (red) circles indicate critical points at which the homogeneous mixture enters the region of both dynamical and mechanical stability.

For temperatures $T > T_{c,\mathrm{mix}}$ before the onset of BCS superfluidity, $\Delta = 0$ and hence we are confined to the n_b axis. Correspondingly, the free energy and the stability conditions of the homogeneous Bose-Fermi mixture are given by simply substituting $\Delta = 0$ in Eqs. (9)-(15). For the parameter space under investigation, we find that the homogeneous mixture is always the stable ground state in this temperature regime. On the other hand, at temperatures $T < T_{c,\mathrm{mix}}$, the onset of BCS superfluidity in fermions is characterized by a non-zero value of Δ. In Fig. 3, we plot the phase diagram for a wide range of temperatures below T_c to observe that the mixture is dynamically stable only above the solid (green) curves at a given temperature. Thus the presence of an all-stable homogeneous phase above $T_{c,\mathrm{mix}}$ and a mixture of unstable/stable phases below $T_{c,\mathrm{mix}}$, as seen in Fig. 3, depicts the unambiguous manifestation of $S_1 \to U_2 \to S_2$ transitions.

Now we can immediately recognize the significance of this phase diagram for a realistic experimental situation. Again, just like the $T = 0$ case, only a small part of the stable phase space, corresponding to a fixed value of λ_f, is accessible in a particular experimental realization. This we indicate by the two-dimensional surface shown in Fig. 3, for our chosen value of λ_f such that the fermions are in the BCS superfluid regime. The dashed lines C_i's are contours connecting phase space points on this surface with fixed temperatures T_i's. The crossing of contours C_i's with dynamical stability contours indicates the phase space points at which the mixture enters the dynamically stable region. The filled circles represent critical points at which the homogeneous Bose-Fermi superfluid mixture becomes the stable ground state, i.e., both dynamically and mechanically stable. We observe their occurrence to transpire in two different ways: (1) In C_1-C_4, critical points occur in the dynamically stable region where the mixture also attains mechanical stability (as illustrated in Sec. III A). (2) Along C_5 (C_6), the BCS transition temperature monotonously reduces with Δ by such an extent that when $\Delta \to 0$, $T_{c,\mathrm{mix}} < T_5$ (T_6). However as discussed before, the mixture is always the stable ground state for $T_{c,\mathrm{mix}} < T$. Hence in C_5-C_6, the critical points are given by their intersections with Δ=0 plane. Thus along each C_i, below these critical points the homogeneous mixture becomes dynamically and/or mechanically unstable. We further find that in the unstable regions, pure fermions phase separate from the mixture. Thus in Fig. 3 we clearly demonstrate the occurrence of temperature-driven mixing-demixing transitions at fixed interaction strengths.

IV. TRAP PROFILES WITHIN LDA

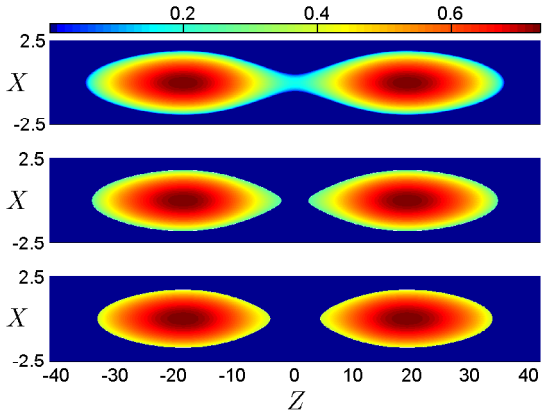

FIG. 4: (Color online) Subplots top, middle and bottom show boson density profiles (slice along y=0 plane) computed within the LDA for temperatures $T = 0.13,\ 0.072,\ 0.055\ T_f$ respectively, with T_c=0.11 T_f. μ_b is adjusted to ensure number conservation (∼42000 atoms). X, Z are in μm. Color bar shows density variations in scale of $n_b a_b^3$ (10^{-6}). Chosen trap parameters V_0 (several mW), σ=12 μm and $\omega_z/\omega_\perp$=0.08.

We now show the direct experimental implications of the above phase stability analysis. This, we do by reliably translating this analysis to the inhomogeneous case via Local Density Approximation (LDA) by defining a position dependent chemical potential $\mu_b(\mathbf{r}) = \mu_b - V_{\mathrm{trap}}(\mathbf{r})$, where $\mu_b(\mathbf{r})$ is the local chemical potential and $V_{\mathrm{trap}}(\mathbf{r})$ is the trap potential for bosons [2]. While this approximation is known to be very efficient for large densities

(typically the case in trapped-atom experiments), it also implies that the trap potential can simultaneously accommodate one or more of the phases discussed above. Thus, remarkably what phase/phases will be observed will critically depend on the trap geometry. This in fact, is a very important observation implying the possibility of tuning the trap parameters such that a desired density profile is observed only if a certain phase has nucleated.

To illustrate this program, let us consider bosons to be in a tightly confined trap surrounded by the Fermi gas in a larger trap, a scenario that takes advantage of our framework to consider a homogeneous Fermi gas with fixed μ_f. Additionally, this consideration is completely justified as the trapping potential for each species can be independently controlled [7]. After careful analysis of the phase diagram in Fig. 3, we find it advantageous to confine bosons in a trap with a finite barrier near the center. As this also helps to enhance the contrast in imaging the nucleated phases, we propose a double-well cigar shaped trap with a potential

$$V_{\rm trap}(\mathbf{r}) = \frac{1}{2}m\omega_\perp(x^2+y^2) + \frac{1}{2}m\omega_z z^2 + V_0\exp(-\frac{z^2}{2\sigma^2})$$

to confine bosons, where $\omega_\perp$ (ω_z) is the trap frequency in the transverse (longitudinal) direction to the Gaussian beam creating the trapping potential. V_0 and σ, defining the barrier peak and beam-width respectively, are chosen to ensure a readily detectable overlap of boson density profiles from the two wells for $T = 0.13\,T_f$ (i.e., $T_c < T$), as shown in the top plot of Fig. 4. At $T = 0.072\,T_f$ ($0.055\,T_f$), phase stability analysis along contour C_5 (C_3) in Fig. 3 indicates the existence of a critical boson density (and correspondingly a critical boson chemical potential $\mu_b(r)$), only above which the Bose-Fermi mixture homogeneously co-exists as the stable ground state. Corresponding regions of the trap where this condition is not satisfied are devoid of bosons in a drastic fashion, as seen from the $\sim$4 μm (8 μm) gap between the separated bosonic islands in Fig. 4. As these separation lengths are far greater than the healing length of the condensate, this illustration vividly shows how crucial aspects of the finite temperature phase diagram readily translate into detectable signatures in experiments. Furthermore, this particular signature in Fig. 4 may be used as a signal indicating the onset of BCS superfluidity in the particular parameter regime of the attractive Fermi gas.

V. EFFECT OF DIMENSIONALITY ON THE PHASE DIAGRAM

As a final piece, we analyze how the phase diagram gets modified when only the trap geometry of the experimental setup is deformed (all other parameters kept constant) such that the confinement in two orthogonal directions is made much tighter compared to that in the third. In effect, the system can be considered to be one-dimensional if the trapping frequency in the tight directions is such that $\hbar\,\omega_{\rm tight} \gg \mu_{b,f}$. For simplicity, we restrict ourselves to the $T = 0$ limit, where all the qualitative features can be comprehensively discussed [23]. The effective 1-d interaction strength can be written in terms of the 1-d scattering length, which in turn can be easily related to the 3-d scattering length [24]. This mapping is critically dependent on the aspect ratio of the trap. We choose experimentally relevant values for $\omega_\perp$ and ω_z [25]. While we assume $\omega_\perp \simeq 2\,\pi\,10^5$ Hz for both bosons and fermions, we find it useful to consider $\omega_\perp/\omega_z \simeq 10^3$ for fermions but smaller values of $\omega_\perp/\omega_z$ for bosons. Apart from ensuring that we are indeed in the 1-d regime, this choice guarantees a highly elongated trapping potential for fermions. From the parameter values used in deriving the 3-d phase diagram of Fig. 1(a), we obtain the corresponding values for the 1-d scenario [24].

We thus construct the phase diagram of the interacting one dimensional superfluid mixture, by performing the 1-d integrals instead of 3-d in Eqs. (9)-(15). The phase diagram is shown in Fig. 5(a), where the solid (green) curve represents the dynamical stability contour that separates the dynamically unstable region (inside the ellipse) from the dynamically stable region (outside the ellipse). Phase space points that correspond to the fixed value of $\lambda_{1d\,f}$, are shown by the dashed (blue) contour C. The crossing of C and the dynamical stability contours indicates the point at which the homogeneous mixture enters the dynamically unstable region. However, as discussed before in Sec. III A, for the Bose-Fermi homogeneous mixture to be stable, it is necessary that the mechanical stability condition be simultaneously satisfied. For this, we plot the relevant free energies in Fig. 5(b), where the free energies of pure bosons, homogeneous mixture and pure fermions along C are given by dotted, dashed and solid lines respectively. We immediately note that pure fermions can never phase separate out of the mixture, a remarkably different result when compared to the 3-d case [see Fig. 1(b)]. The filled circle (red) represents the critical point along contour C, at which the free energy of the bosons becomes lower than that of the homogeneous mixture, i.e., the critical point at which the homogeneous mixture becomes mechanically unstable. This means that up until this critical point, homogeneous superfluid mixture coexists as the stable ground state. However, above this critical point pure bosons phase separate out of the mixture. The significance of this critical point is clear since we can now directly obtain the boson density profile in the boson trap by mapping the boson chemical potential $\mu_b[C]$ onto the spatial coordinate in the trap via LDA using $\mu_b[C] = \mu_b(r) = \mu_b - V(r[C])$, where $V(r)$ is the probe trapping potential for the bosons. It is evident from Figs. 5(a) and 5(b) that the pure bosons phase separate out of the homogeneous mixture in the trap above the critical value of boson chemical potential μ_b corresponding to the critical point (filled red circle).

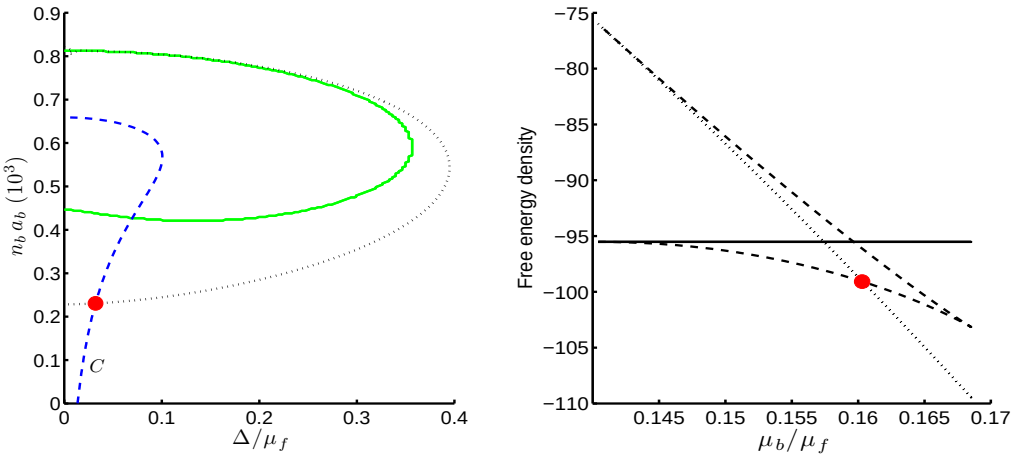

FIG. 5: (Color online) (a) Phase diagram of the Bose-Fermi superfluid mixture in 1-d at $T = 0$ (for the same parameters used in Fig. 1(a)). Solid (green) curve is the dynamical stability contour, while the dashed (blue) contour C denotes phase space points with a fixed value of $\lambda_{1D\,f}$. The dotted (black) curve represents the region within which the homogeneous mixture is mechanically unstable. The filled circle (red) represents the critical point, for this specific experimental realization, at which the homogeneous mixture enters the mechanically unstable region. (b) Plot of the free energy densities of pure bosons (dotted), of pure fermions (solid) and the homogeneous mixture (dashed) against $\mu_b[C]$. Free energy density of homogeneous mixture becomes higher than that of pure bosons at the critical point represented by the filled (red) circle, resulting in the phase separation of pure bosons out of the mixture. Here, free energy density is a dimensionless quantity [22].

VI. CONCLUSIONS

In this article, we have discussed a consistent theoretical method for performing the finite temperature phase stability analysis of an ultra-cold mixture comprising of bosons and fermions, both in the superfluid regime. Based on our stability analysis in the vicinity of the Fermi superfluid temperature, we discussed two distinct scenarios where the homogeneous superfluid mixture becomes unstable (1) when the normal-superfluid phase transition (second-order) occurs in the fermionic component, and (2) below the Fermi superfluid temperature via mechanical instability which is a first-order phase-separation phase transition. The latter scenario happens exclusively due to the trap inhomogeneity inherent in trapped-atom experiments, thereby allowing for the two phases to be simultaneously present. We have illustrated the emergence of these instabilities and the ensuing phase separation by considering a realistic experimental setting. We fine-tuned the trap geometry to enhance the effect of phase separation. Finally, we briefly discussed the effect of dimensionality on the stability of various phases. We reiterate that while our phase diagram analysis is quantitatively exact when the interactions are weak, our study is only qualitatively correct in the strong interaction limit.

We emphasize here that the interplay between the first and second order phase transitions, similar to that discussed in this paper, will have strong implications for analyzing experimental observations involving ultra-cold mixtures in general [26]. While our framework is also valid to study the regime of strong interactions near a broad Feshbach resonance, it can be easily extended within a two channel model for the case of a narrow Feshbach resonance. Further, while such a treatment will naturally allow for a molecular condensate of Fermi atoms [27], it is not hard to speculate emergence of rich physics due to occurrence of Efimov bound states in the Bose-molecule interaction channel [28]. Finally, an important extension of the current work would be to consider spin-dependent Bose-Fermi interactions. The presence of a small BEC can shift the chemical potential of a particular spin component relative to the other. This is analogous to the situation encountered in solid-state samples with magnetic impurities, thereby providing a new platform for studying the interplay between superfluidity and magnetism.

Acknowledgments

This work is supported by the W. M. Keck Program in Quantum Materials at Rice University, NSF, and the Robert A. Welch Foundation (Grant No. C-1669). S.B. also acknowledges funding from the Centre for Quantum Science at George Mason University.

[1] I. Bloch *et al.*, Rev. Mod. Phys. **80**, 885 (2008)

[2] C. J. Pethick and H. Smith, *Bose-Einstein Condensation in Dilute Gases* (Cambridge University Press, 2001)

[3] M. Inguscio, W. Ketterle and C. Salomon, *Ultra-cold Fermi Gases* (IOS Press, Amsterdam, 2008)

[4] E. Wille *et al.*, Phys. Rev. Lett. **100**, 053201 (2008); K. Pilch *et al.*, Phys. Rev. A, **79**, 042718 (2009)

[5] R. Ciurylo *et al.*, Phys. Rev. A **71**, 030701(R) (2005); K. Enomoto *et al.*, Phys. Rev. Lett. **101**, 203201 (2008); Y. N. Martinez de Escobar *et al.*, arXiv:0906.1837.

[6] M. Greiner *et al.*, Nature **415**, 39 (2002)

[7] Z. Hadzibabic *et al.*, Phys. Rev. Lett. **88**, 160401 (2002); *ibid.* **91**, 160401 (2003)

[8] S. Inouye *et al.*, Phys. Rev. Lett. **93**, 183201 (2004); M. Zaccanti *et al.*, Phys. Rev. A, **74**, 041605 (2006)

[9] K. Maeda *et al.*, Phys. Rev. Lett. **103**, 085301 (2009)

[10] Experimental realization has not been possible due to extremely low superfluid transition temperature of ^{3}He.

[11] An interesting proposal to make $T_c > T_{BEC}$ is considered in R. Onofrio *et al.*, Phys. Rev. Lett. **89**, 100401 (2002)

[12] C. Chin *et al.*, Science **305**, 1131 (2004)

[13] M. Holland *et al.*, Phys. Rev. Lett. **87**, 120406 (2001)

[14] For diagonalizing the mean-field Hamiltonian, we closely follow the arguments presented in A. Altland and B. Simons, *Condensed Matter Field Theory* (Cambridge University Press, 2006)

[15] Even if Δ is not real and $\Delta = |\Delta|e^{i\phi}$, it can always be made real by the global gauge transformation [14].

[16] Daw-Wei Wang, Phys. Rev. Lett. **96**, 140404 (2006).

[17] S. G. Bhongale *et al.*, Phys. Rev. A **78**, 061606(R) (2008).

[18] This choice is especially useful if we consider the bosons to be in a tight trap enclosed by the fermions in a larger trap.

[19] In 3-d, the term $\sum_k (\xi_k - E_k)$ itself diverges and hence it is useful to add the term $\sum_k \Delta^2/2\,\varepsilon_k$. At equilibrium, the absolute value of free energy f remains unchanged due to regularization, since we have simply included terms $+\sum_k \Delta^2/2\,\varepsilon_k$ in $\sum_k (\xi_k - E_k)$ and $-\sum_k \Delta^2/2\,\varepsilon_k$ in $\Delta^2/|\lambda_f|$.

[20] For the given range of λ_f, mean-field treatment overestimates T_c by about a factor of 2 as shown in Phys. Rev. A **75**, 023610 (2007) and Phys. Rev. Lett. **71**, 3202 (1993). However, Phys. Rev. Lett. **101**, 070404 (2008) reports achieving temperatures $T < 0.05\,T_f$. For the given value of $1/k_f a = -1.1$, the actual critical temperature, T_c, is definitely greater than $0.05\,T_f$ and hence represents a scenario already realized in current experiments.

[21] Here, chosen values are: T_f=μ_f/k_B=3.8 μK (m=6 amu), a_b=35 a_0 and a_{bf}=230 a_0, where a_0 is the Bohr radius and μ_f is fixed in our analysis.

[22] Free energy density is made dimensionless by scaling with respect to the energy density of a 3-d non-interacting gas occupying a volume of $1/k_f^3$ with fermi-momentum $k_f = 1/3200\,a_0$ and $m = 6\,amu$. Corresponding vales in the 1-d limit are computed using the results in [24].

[23] Phase diagram of the Bose-Fermi superfluid mixture in 1-d at $T = 0$ was already discussed by two authors of this manuscript in Ref. [17].

[24] M. Olshanii, Phys. Rev. Lett. **81**, 938 (1998). Also, we assume here that the regularization performed in determining fermion-fermion interaction strength λ_f in 3-d has no effect on the corresponding 1-d effective strength $\lambda_{1d\,f}$.

[25] Say, as mentioned in Y.-a. Liao *et al.*, Nature, **467**, 567 (2010)

[26] Since the submission of our manuscript, very recent theoretical work by Leslie O. Baksmaty *et al.,* [arXiv:1003.4488] (to appear in Phys. Rev. A) based on extensive numerical calculation has confirmed a crucial role played by condensate nucleation and the resulting phase separation in a polarized Fermi gas. In this paper, the authors attribute such non-homogeneous nucleation as an explanation to the controversy between the MIT and Rice polarized Fermi gas experiments reported in Science **311**, 492 (2006) and Science **311**, 503 (2006) respectively.

[27] M. Greiner *et al.*, Nature, **426**, 537 (2003)

[28] T. Kraemer *et al.*, Nature, **440**, 315 (2006); E. Braaten *et al.*, Annals of Physics, **322**, 120 (2007)